Emission properties and energy transfer in Perylene-Rhodamine 6 G co-doped polymeric fiber

P. Miluski*, M. Kochanowicz, J. Żmojda, and D. Dorosz

Bialystok University of Technology, Wiejska 45D Street, Bialystok 15-351, Poland
**Corresponding author: p.miluski@pb.edu.pl*

Received July 22, 2016; accepted October 28, 2016; posted online November 22, 2016

This Letter presents the fabrication and characterization of a perylene (Per) and Rhodamine 6 G (Rh 6 G) co-doped polymeric fiber. The spectroscopic properties (luminescence spectra, attenuation, energy transfer) of the co-doped polymethyl methacrylate (PMMA) fiber are presented. Two different concentrations of Rh 6 G (2.2×10^{-4} and 4.1×10^{-4} mol/L) and a constant Per concentration (6.2×10^{-4} mol/L) are used in the experiments. The luminescence spectrum changes versus the fiber length are discussed. Additionally, the ratio of the maximum fluorescence peaks of the used dyes is calculated versus the fiber length. The obtained results show the energy transfer from Per (donor) to Rh 6 G (acceptor). The proposed co-doped fiber can be used in applications in lighting and sensor technology.

OCIS codes: 160.4890, 160.2540, 160.5470.
doi: 10.3788/COL201614.121602.

Numerous applications of luminescent inorganic glasses doped with lanthanides have been reported in the literature[1–9]. They ensure stable luminescent properties and can be applied in glass optical fiber technology[10–13]. In contrast to rare earth, organic dyes exhibit typically brighter luminescence and significantly higher absorption and emission cross sections[14]. Additionally, organic dyes can be easily incorporated into polymeric hosts, which are widely used in optoelectronic devices. The most frequently used kind of polymer is polymethyl methacrylate (PMMA), as it assures excellent optical properties in the visible spectral range. Moreover, the polymeric optical fiber's drawing temperature is acceptable for organic dyes. It is highly important to prevent their degradation or fiber breakdown during the fabrication process. Several different optical fiber preform fabrication processes (co-polymerization, drilling, rotational polymerization) can be applied in organic optical fiber technology, which allows researchers to obtain complex refractive indexes (step index, gradient index, capillary, photonic band gap) and dopant distribution profiles[15–18]. There are numerous application of polymeric fibers, and among them, luminescent polymer optical fibers have been used as scintillators, optical fiber amplifiers, lasers, and sensors[19–26]. The optical radiation amplification and spectroscopic properties of single dye-doped polymer optical fibers have been studied, showing potential applications in optical fiber technology[19,20]. However, co-doped polymeric systems can significantly extend these applications fields, particularly in terms of the energy exchange phenomenon between molecules in a liquid and a solid organic host[27,28]. This is known as the fluorescence resonant energy transfer (FRET) and is used in fluorescence-based microscopy and sensor applications[29,30]. Among the different xanthene organic dyes, Rhodamine 6 G (Rh 6 G) is one of the most efficient. Its fluorescence at $\lambda_{max} = 552$ nm additionally lies in low-loss window of PMMA. Other advantages, such as high quantum yield (0.95) and reasonable luminescence quenching levels at high energy excitations, are useful in numerous optical fiber amplifiers and lasers constructions[14,20]. The other dye, perylene (Per), is a polycyclic aromatic hydrocarbon with an intense luminescence at $\lambda_{max} = 446$ nm. The quantum yield has been reported to be 0.94[31]. Moreover, the low photobleaching effect, efficient carrier mobility, and good processability make Per one of the most important dyes in OLED technology. Its derivatives allow researchers to also obtain green, orange, and red luminescence[32,33]. These dyes can be incorporated into PMMA using a solvent-free technique, which assures a low level of undesired residues in polymeric optical fiber preforms. The luminescence properties (gain, laser action condition, spectra shifts) of Per and Rh 6 G, by using down- and upconversion mechanisms, can be obtained in the organic host[34]. In this Letter, the chosen pair of organic dyes allows the investigation of the down energy transfer between luminescent organic molecules. The wide overlap spectrum (c.a. 450–550 nm) of luminescence of Per (donor) and Rh 6 G's (acceptor) absorbance spectra allows us to obtain an efficient energy transfer. The absorption and emission spectra of the used dyes were reported in the literature[35,36]. The light-guiding mechanism of the optical fiber structure shows unique properties of spectra behaviors in comparison with the limited-thickness bulk samples. The cylindrical fiber structure extends the affecting length of the excitation radiation and energy exchange process. The results obtained in the Letter show that the energy transfer process occurs for short distances of polymer fibers. Although the fluorescence energy transfer in a donor–acceptor pair was reported in the literature[28–30], the strongly limited number of published results of energy transfer (radiative and nonradiative) in co-doped polymeric optical fibers shows the necessity of further investigations in this field.

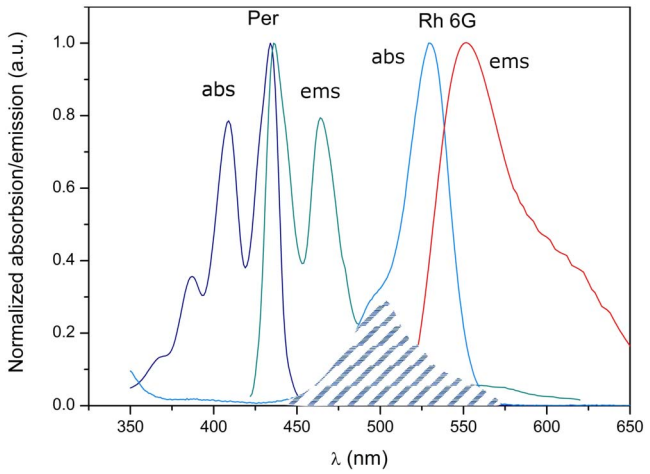

Fig. 1. Normalized absorption/emission spectra of Per (donor) and Rh 6 G (acceptor)[37].

The obtained luminescence spectra show different properties for short and long fibers. Typically, the emission peaks of Per are located at 499, 464, and 436 nm (Fig. 1). They can be observed in the luminescence spectrum of the PMMA bulk sample (Fig. 1). The emission (Per, donor) and absorption (Rh 6 G, acceptor) spectra overlap (marked on Fig. 1), which can affect the energy transfer between these dyes.

The energy level system of the co-doped Per (donor)-Rh 6 G (acceptor) system with a possible energy transfer (k_{ET}) is presented in Fig. 2, where σ_p^a is the absorption cross section at the pump wavelength, σ_s^a is the absorption cross section at the signal (luminescence) wavelength, σ_p^e is the emission cross section at the signal wavelength, τ is lifetime of level 2, and τ_v is the lifetime of level 3 (the Per and Rh 6 G coefficients are indexed 1 and 2, respectively).The total energy transfer can be calculated using[28]

$$\eta = 1 - \frac{I_d}{I_{od}}, \tag{1}$$

where I_{od} is the fluorescence intensity of the donor, and I_d is the fluorescence intensity of the donor at the considered fiber length.

The PMMA-doped preform was fabricated using the free-radical polymerization method. The raw materials, luminescent organics (Per, Rh 6 G), methyl methacrylate (MMA), benzoyl peroxide (BP), and butanethiol (B), were supplied by Sigma-Aldrich with purities above 99%. The polymer preform fabrication process was performed according to the process presented in the literature[16,26].

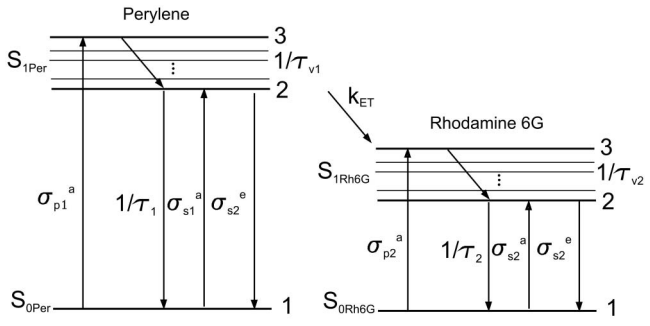

Fig. 2. Energy level system of co-doped Per-Rh 6 G system.

The two different ratio of Rh 6 G were used for the energy transfer investigation. The Per concentration 6.2×10^{-4} mol/L was kept constant, while the Rh 6 G concentration was 2.2×10^{-4} and 4.1×10^{-4} mol/L for preforms A and B, respectively. The used acceptor concentrations were chosen because they ensure bright (no self-quenching) luminescence in PMMA fibers. The significant acceptor concentration on the spectroscopic properties of organic dye-doped PMMA fibers will be presented. The obtained preforms were uniform and transparent, without any visible defects (bubbles or cracks). The fibers were fabricated using a computer-controlled drawing process. The main process parameters were as follows: furnace temperatures $T = 160$°C–185°C, preform feeding 0.5–0.6 cm/min, and drawing speed 60–300 cm/min. The experiments show a good stability of the drawing of fabricated preforms. Few tenth of meters of good-quality (exact cylindrical shape, and no visible defects) PMMA fibers were fabricated with diameters in the range from 0.2–2.0 mm. This confirms the proper drawing parameters were used. The spectroscopic investigation was performed using 0.8 mm diameter fibers, as these ensure effective pump-power coupling. Additionally, the pump power density has to be limited, since the glass transition temperature (c.a. 105°C) is much lower in comparison with that of the optical glass fibers. The photos of the preforms and the polymer fiber used for the measurements are presented in Fig. 3. The attenuation was measured using a halogen Stellarnet SL1 lamp and a Stellarnet Green Wave spectrometer in the range of 400–900 nm at a 0.5 nm resolution. The cutback method was used for optical fiber characterization by direct face excitation of the polymer fiber. Additionally, the microscopic objective was used to ensure the efficient coupling of the excitation radiation into the fiber. The luminescent properties were measured using a laser diode (405 nm, 200 mW, current regulated). The optical fiber-coupled Stellarnet Green Wave spectrometer at a 0.5 nm resolution was used for signal

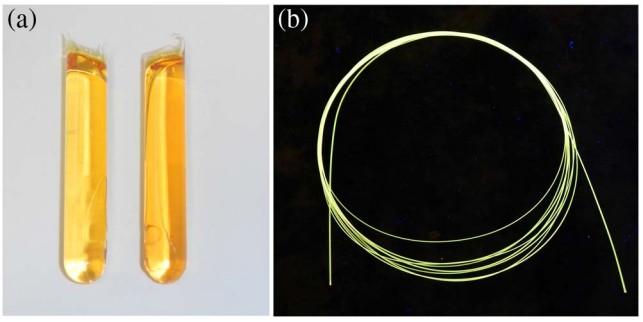

Fig. 3. Photos of (a) Per-Rh 6 G co-doped preforms and (b) fiber fabricated from preform A under UV (365 nm) excitation.

detection at the end face of the optical fiber. The scheme of the measurement setup is presented in Fig. 4.

In a waveguideing structure, such as a polymeric fiber, the dominant luminescence peak of Per is 464 nm because of the strong reabsorption effects (Fig. 5). The maximum of the luminescence peak for Rh 6 G can be observed at 583 nm. Additionally, the spectrum shape modification can be noticed for fiber lengths up to 50 mm. The analysis of the short-length fibers shows the fluorescence spectra of both dyes incorporated into the PMMA fiber. For longer fibers (>40 mm), the Rh 6 G luminescence is dominant. The energy transfer between the Per and Rh 6 G molecules is noticeable then (Fig. 5). The dominant parameter for spectrum shape changes in the energy transfer process between Per (donor) and Rh 6 G (acceptor) and is the overlap emission and absorption spectra of the used dyes.

It is clear that the whole energy transfer occurs over a distance of 0.05 m. Moreover, the reabsorption of the luminescence of the Per by Rh 6 G strongly depends on the concentration of the acceptor (the energy efficiency for smaller distances is higher for Rh 6 G the concentration of 4.1×10^{-4} mol/L, as presented in Fig. 6). In such circumstances, the spectrum shift $\lambda_{\max}$ can be observed for the Per and Rh 6 G fluorescence peaks. The red-shifts of the luminescence spectra of Per and Rh 6 G (Fig. 7) are caused by reabsorption effects in the mixed dye-doped fiber. The higher concentration of the acceptor allows more noticeable fluorescence reabsorption in polymeric fiber structures. Moreover, the luminescence efficiency of the Rh 6 G dye depends on direct excitation by laser radiation and donor emission, in contrast to Per, which can be excited only by a laser diode (405 nm). It is obvious that the pump-power intensity changes versus the fiber length can be used for spectral shape modification. The emission spectrum shift that is also a result of the energy transfer process changes for different lengths of the fiber as the overlap of the emission and absorption spectra also varies. The spectral red-shift phenomenon of the Rh 6 G dye in a waveguiding polymeric structure is dominant for longer fibers. The measurements have shown that the most effective pumping lengths are 50 and 70 mm (fibers A and B, at a 1% initial power criterion). The measurements for long fibers were performed for

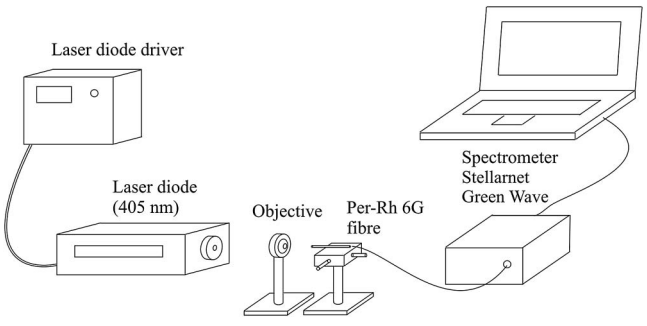

Fig. 4. Scheme of the measurement setup.

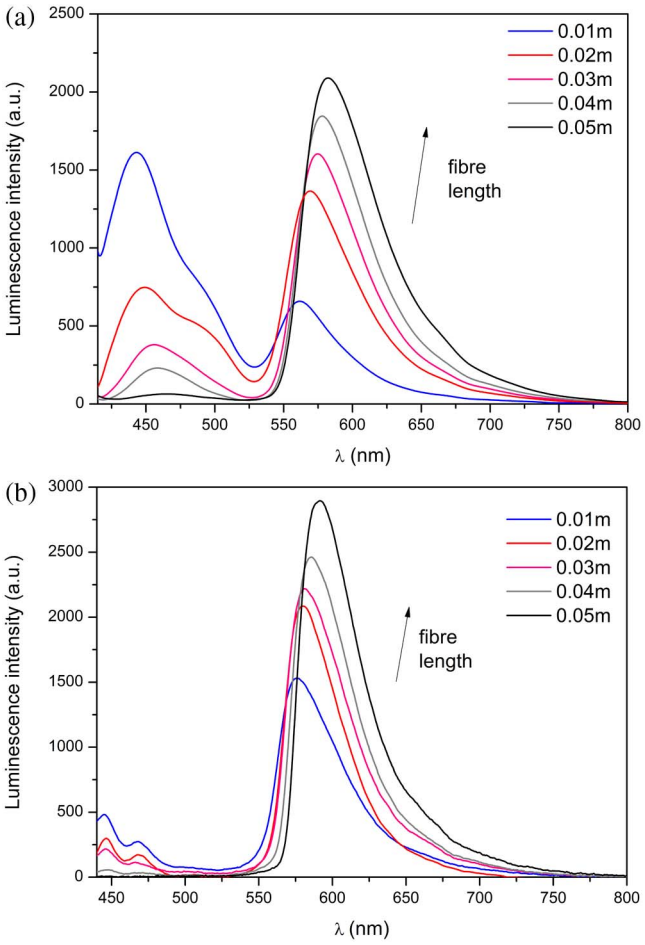

Fig. 5. Luminescence spectra of co-doped fiber fabricated from (a) preform A (Per/Rh6 G ratio 2.8), and (b) preform B (Per/Rh6 G ratio 1.5) viewed during short-length analysis.

distances from 0.05–1.0 m. The attenuation spectra are presented in Fig. 8.

The relatively high level of attenuation is caused by the construction of fiber (air cladding structure). It is also significantly higher than that in commercially available

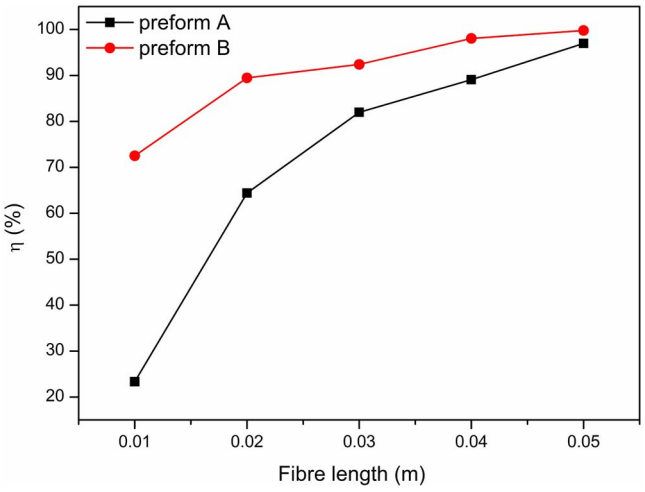

Fig. 6. Energy transfer (Per-Rh6 G) efficiency ratio versus the fiber length.

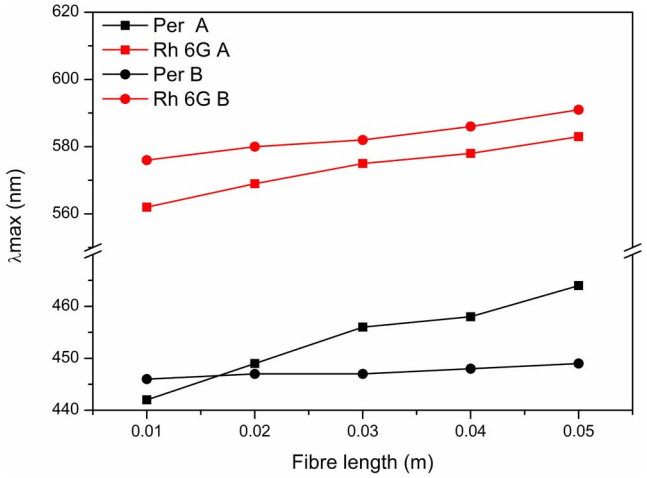

Fig. 7. λ_{max} shift of Per and Rh 6 G dye in fabricated fibers.

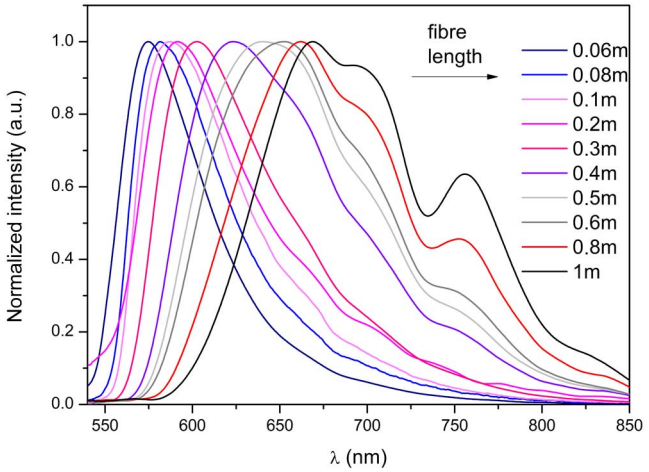

Fig. 9. Normalized emission spectra of co-doped fiber fabricated from preform A.

polymer step index optical fibers. The high attenuation (above 3 dB/cm) for wavelengths below 600 nm is caused by the absorption of the radiation by the organic dyes. The emission of the Per fades out for distances shorter than 0.05 m. The emission spectra of Per cannot be seen, since the strong (Rh 6 G) acceptor absorption effectively decreases it for distances smaller than 0.05 m. The normalized emission spectra are presented in Figs. 9 and 10. The spectral red-shift phenomenon in the λ_{max} range over 80 nm can be noticed. The detailed λ_{max} and full width at half-maximum (FWHM) for the fibers fabricated from preforms A and B are illustrated in Fig. 11. The spectrum shape for long-distance fibers becomes wider, but the intensity of the main fluorescence peak decreases significantly. The red-shift of the luminescence spectrum (reabsorption) and the spectral attenuation cause decreasing fluorescence intensity versus the fiber length. The broadening of the luminescence peak corresponds to a nonsymmetrical luminescence peak. The long right-side tail is visible in emission spectra of Rh 6 G (Fig. 1). In fact, additional spectral attenuation of the polymeric host

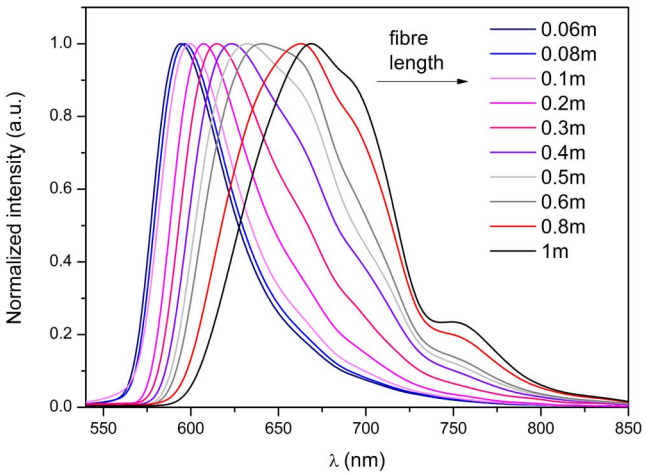

Fig. 10. Normalized emission spectra of co-doped fiber fabricated from preform B.

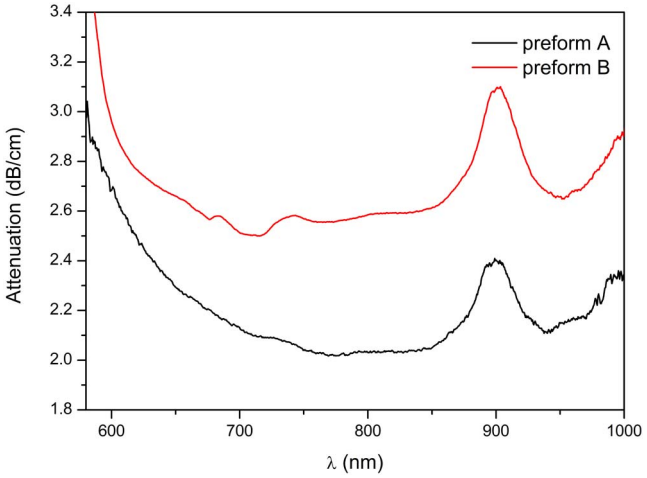

Fig. 8. Attenuation spectra of co-doped fabricated fibers A and B.

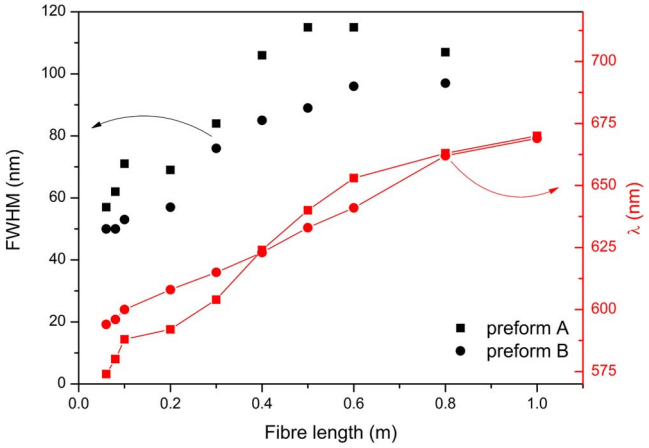

Fig. 11. FWHM of luminescence spectrum and λ_{max} shift versus fiber length.

causes the spectrum at the end face of the fiber to significantly differ from the luminescence spectra of the used dyes.

The energy transfer in the presented co-doped polymeric fibers can be noticed over the relatively short distances (shorter than 0.05 m). The analysis for long-length fibers shows a lack of luminescence, which is expected for the Per dye. The dominant role in the realized energy transfer is played by the fluorescence of the Rh 6 G molecules. The interesting properties of the spectral behaviors (red-shift, spectrum shape changes) of co-doped polymerics are caused mostly by reabsorption processes for the long optical radiation path in the PMMA fiber. For distances longer than 0.05 m, the Rh 6 G spectral red-shifts over 80 nm, and shape changes is presented. Moreover, additional spectral attenuation of the polymeric host causes the spectrum at the end face of fiber to significantly differ from the luminescence spectra of the used dyes. The spectroscopic properties, e.g., efficient fluorescence and spectrum shape modification, presented in this Letter can be applied in new optical fiber constructions. Dye mixture-doped polymer optical fibers can be applied in compact light sources and broad-wavelength optical amplifiers.

This work was supported by Bialystok University of Technology (Project No. S/WE/4/2013).

References

1. F. Auzel and P. Goldner, Opt. Mater. **16**, 93 (2001).
2. L. C. V. Rodrigues, H. F. Brito, J. Hölsä, and M. Lastusaari, Opt. Mater. Express **2**, 382 (2012).
3. M. Kochanowicz, D. Dorosz, J. Zmojda, P. Miluski, and J. Dorosz, Acta Phys. Polonica A **124**, 471 (2013).
4. P. S. Peijzela, A. Meijerinka, R. T. Wegha, M. F. Reidb, and G. W. Burdick, J. Solid State Chem. **178**, 448 (2005).
5. B. Burtan, M. Reben, J. Cisowski, J. Wasylak, N. Nosidlak, J. Jaglarz, and B. Jarząbek, Acta Phys. Polonica A **120**, 579 (2011).
6. C. Joshi and S. Rai, J. Quantum Spectrosc. Radiative Transfer **113**, 397 (2012).
7. X. Feng, C. H. Qi, F. Y. Lin, and H. F. Hu, J. Non-Cryst. Solids **257**, 372 (1999).
8. Q. Liu, B. F. Johnston, S. Gross, M. J. Withford, and M. J. Steel, Opt. Mater. Express **3**, 2096 (2013).
9. M. Kochanowicz, D. Dorosz, J. Zmojda, and J. Dorosz, Acta Phys. Polonica A **122**, 837 (2012).
10. O. N. Egorova, S. L. Semjonov, V. V. Velmiskin, Y. P. Yatsenko, S. E. Sverchkov, B. I. Galagan, B. I. Denker, and E. M. Dianov, Opt. Express **22**, 7632 (2014).
11. Y. W. Lee, S. Sinha, M. J. F. Digonnet, and R. L. Byer, Opt. Lett. **31**, 3255 (2006).
12. M. Kochanowicz, J. Zmojda, P. Miluski, J. Pisarska, W. A. Pisarski, and D. Dorosz, Opt. Mater. Express **5**, 1505 (2015).
13. A. Mafi, J. V. Moloney, D. Kouznetsov, A. Schülzgen, S. Jiang, T. Luo, and N. Peyghambarian, IEEE Photon. Technol. Lett. **16**, 2595 (2004).
14. J. Arrue, F. Jiménez, I. Ayesta, M. Asunción Illarramendi, and J. Zubia, Polymers **3**, 1162 (2011).
15. M. Kailasnatha, T. S. Sreejayaa, R. Kumar, C. P. G. Vallabhanb, V. P. N. Nampooria, and P. Radhakrishnana, Opt. Laser Technol. **40**, 687 (2008).
16. R. Oliveira, L. Bilro, and R. Nogueira, Appl. Opt. **54**, 5629 (2015).
17. Y. Huang, Y. Xu, and A. Yariv, Appl. Phys. Lett. **85**, 5182 (2004).
18. G. Barton, M. A. Eijkelenborg, G. Henry, M. C. J. Large, and J. Zagari, Opt. Fiber Technol. **10**, 325 (2004).
19. M. Karimi, N. Granpayeh, and M. K. Morraveg Frshi, Appl. Phys. B **78**, 387 (2004).
20. I. Ayesta, J. Arrue, F. Jiménez, M. Asunción Illarramendi, and J. Zubia, J. Lightwave Technol. **29**, 2629 (2011).
21. H. Y. Tama, J. P. Chi-Fung, G. Zhou, X. Cheng, and M. L. V. Tse, Opt. Fiber Technol. **16**, 357 (2010).
22. L. Bilro, N. Alberto, J. L. Pinto, and R. Nogueira, Sensors **12**, 12184 (2012).
23. C. Baleizao, S. Nagl, M. Schaferling, M. N. Berberan-Santos, and O. S. Wolfbeis, Anal. Chem. **80**, 6449 (2008).
24. P. Miluski, D. Dorosz, M. Kochanowicz, and J. Żmojda, Proc. SPIE **8903**, 89030C (2013).
25. P. Miluski, D. Dorosz, M. Kochanowicz, J. Zmojda, and J. Dorosz, Proc. SPIE 981607 (2015).
26. P. Miluski, D. Dorosz, J. Zmojda, M. Kochanowicz, and J. Dorosz, Acta Phys. Polonica A **127**, 730 (2015).
27. N. R. Tanzeela and M. R. Brouwer, "Fluorescence spectroscopy in polymer science," in *Advanced Fluorescence Reporters in Chemistry and Biology III* (Springer-Verlag, 2011).
28. M. Kailasnatha, N. Kumarb, V. P. N. Nampooria, C. P. G. Vallabhanb, and P. Radhakrishnana, J. Photochem. Photobiol. A: Chem. **199**, 236 (2008).
29. L. Lindenburg and M. Merkx, Sensors **14**, 11691 (2014).
30. N. Polleya, S. Singha, A. Giri, P. K. Mondal, P. Lemmens, and S. K. Pal, Sens. Actuators B **210**, 381 (2015).
31. I. B. Berlman, *Handbook of Fluorescence Spectra of Aromatic Molecules* (Academic Press, 1965).
32. C. W. Chang, H. Y. Tsai, and K. Y. Chen, Materials **7**, 5488 (2014).
33. L. B.-A. Johansson, Spectrochimica Acta **47**, 857 (1991).
34. Y. Murakami, Chem. Phys. Lett. **516**, 56 (2011).
35. A. M. Brouwer, Pure Appl. Chem. **83**, 2213 (2011).
36. J. Peter, C. P. G. Vallabhan, P. Radhakrishnan, V. P. N. Nampoori, and M. Kailasnath, Opt. Laser Technol. **63**, 34 (2014).
37. http://www.fluorophores.tugraz.at/, 16.04.2016.